

# Landfast ice thickness in the Canadian Arctic Archipelago from Observations and Models

Stephen. E. L. Howell<sup>1</sup>, Frédéric Laliberté<sup>1</sup>, Ron Kwok<sup>2</sup>, Chris Derksen<sup>1</sup> and Joshua King<sup>1</sup>

<sup>1</sup>Climate Research Division, Environment Canada, Toronto, Canada

<sup>2</sup>Jet Propulsion Laboratory, California Institute of Technology, Pasadena, California, USA

## Abstract

Observed and modelled landfast ice thickness variability and trends spanning more than five decades within the Canadian Arctic Archipelago (CAA) are summarized. The observed sites (Cambridge Bay, Resolute, Eureka and Alert) represent some of the Arctic's longest records of landfast ice thickness. Observed end-of-winter (maximum) trends of landfast ice thickness (1957-2014) were statistically significant at Cambridge Bay ( $-4.31 \pm 1.4$  cm decade<sup>-1</sup>), Eureka ( $-4.65 \pm 1.7$  cm decade<sup>-1</sup>) and Alert ( $-4.44 \pm 1.6$  cm decade<sup>-1</sup>) but not at Resolute. Over the 50+ year record, the ice thinned by  $\sim 0.24$ - $0.26$  m at Cambridge Bay, Eureka and Alert with essentially negligible change at Resolute. Although statistically significant warming in spring and fall was present at all sites, only low correlations between temperature and maximum ice thickness were present; snow depth was found to be more strongly associated with the negative ice thickness trends. Comparison with multi-model simulations from Coupled Model Intercomparison project phase 5 (CMIP5), Ocean Reanalysis Intercomparison (ORA-IP) and Pan-Arctic Ice-Ocean Modeling and Assimilation System (PIOMAS) show that although a subset of current generation models have a 'reasonable' climatological representation of landfast ice thickness and distribution within the CAA, trends are unrealistic and far exceed observations by up to two orders of magnitude. ORA-IP models were found to have positive correlations between temperature and ice thickness over the CAA, a feature that is inconsistent with both observations and coupled models from CMIP5.

24

## 25 **1. Introduction**

26           The World Meteorological Organization (WMO, 1970) defines landfast sea ice as “sea  
27 ice which remains fast along the coast, where it is attached to the shore, to an ice wall, to an ice  
28 front, or over shoals, or between grounded icebergs.” In the Arctic, this ice typically extends to  
29 the 20-30 m isobaths [Mahoney *et al.*, 2007; Mahoney *et al.*, 2014]. It melts each summer and  
30 reforms in the fall but there are regions along the northern coast of the Canadian Arctic  
31 Archipelago (CAA) where multi-year landfast ice (also termed an “ice plug”) is present. The two  
32 most prominent regions of multi-year landfast sea ice in the CAA are located in Nansen Sound  
33 and Sverdrup Channel [Serson, 1972; Serson, 1974] (Figure 1). It has been documented that ice  
34 remained intact from 1963-1998 in Nansen Sound and from 1978-1998 in Sverdrup Channel  
35 [Jeffers *et al.*, 2001; Melling, 2002; Alt *et al.*, 2006]. The extreme warm year of 1998  
36 disintegrated the ice in both regions and their survival during the summer melt season in recent  
37 years has occurred less frequently [Alt *et al.*, 2006]. Over the entire Arctic, landfast ice extent is  
38 declining at 7% decade<sup>-1</sup> since the mid-1970s [Yu *et al.*, 2013]

39           Records of landfast ice thickness provide annual measures of ice growth that can also  
40 almost entirely be attributed to atmospheric forcing with negligible deep ocean influence on local  
41 ice formation. While the key forcings on landfast ice and offshore ice are different, the seasonal  
42 behavior of landfast ice can nevertheless provide useful information for understanding the  
43 interannual variability of ice thickness in both regimes. Presently, there is no pan-Arctic network  
44 for monitoring changes in landfast ice but available measurements suggest thinning in recent  
45 years. Thickness measurements near Hopen, Svalbard revealed thinning of landfast ice in the  
46 Barents Sea region by 11 cm decade<sup>-1</sup> between 1966 and 2007 [Gerland *et al.*, 2008]. From a

47 composite time series of landfast ice thickness from 15 stations along the Siberian coast,  
48 *Polyakov et al.* [2010] estimate an average rate of thinning of 3.3 cm decade<sup>-1</sup> between the mid-  
49 1960s and early 2000s. Relatively recent observations by *Mahoney et al.* [2007] and  
50 *Druckenmiller et al.* [2009] found longer ice-free seasons and thinner landfast ice compared to  
51 earlier records.

52 At four sites in the CAA, *Brown and Cote* [1992] (hereinafter, BC92) provided the first  
53 examination of the interannual variability of end-of-winter (maximum) landfast ice thickness and  
54 associated snow depth over the period 1957-1989. Their results highlighted the insulating role of  
55 snow cover in explaining 30-60% of the variance in maximum ice thickness. Similar results were  
56 also reported by *Flato and Brown* [1996] and *Gough et al.* [2004]. In the record examined by  
57 BC92, no evidence for systematic thinning of landfast ice in the CAA was found. Landfast ice  
58 thickness records at several of these CAA sites are now over 50 years in length, which represents  
59 an addition of more than two decades of measurements since BC92 during a period that saw  
60 dramatic reductions in the extent and thickness of Arctic sea ice [e.g. *Kwok and Rothrock*, 2009;  
61 *Stroeve et al.*, 2012].

62 The sparse network of long term observations of snow and ice thickness in the Arctic  
63 (clearly exhibited by only four ongoing measurements sites operated by Environment Canada in  
64 the CAA) has made the use of models imperative to provide a broader regional scale perspective  
65 of sea ice trends in a warming climate. Given the coarse spatial resolution of global climate  
66 models, previous studies focusing on the CAA have relied on either a one-dimensional  
67 thermodynamic dynamic model [*Flato and Brown*, 1996; *Dumas et al.*, 2006] or a regional three-  
68 dimensional ice-ocean coupled model [e.g. *Sou and Flato*, 2009]. Specifically, *Dumas et al.*  
69 [2006] found projected maximum ice thickness decreases of 30 cm by 2041-2060 and 50 cm by

70 2081-2100 and *Flato and Sou* [2009] reported a potential 17% decrease in overall ice thickness  
71 throughout the CAA by 2041-2060. However, in recent years some global climate models,  
72 reanalysis products, and data assimilation systems are now of sufficient spatial resolution to  
73 assess potential landfast ice thickness changes within the CAA.

74 This analysis examines the trends of measured landfast ice thickness, snow depth and air  
75 temperature over a 50+ year period between 1957 and 2014 and compares the results with the  
76 earlier analysis by BC92. We then use this observational foundation to evaluate the  
77 representativeness of landfast ice in state-of-the-art global climate models, assimilation systems  
78 and re-analysis products.

79

## 80 **2. Data Description**

### 81 **2.1. Observations**

82 Landfast ice thickness and corresponding snow depth measurement have been made  
83 regularly at many coastal stations throughout Canada since about 1950. These data are quality  
84 controlled and archived at the Canadian Ice Service (CIS) and represent one of the few available  
85 sources of continuous ice thickness measurements in the Arctic. In general, thickness  
86 measurements are taken once per week, starting after freeze-up when the ice is safe to walk on  
87 and continuing until breakup or when the ice becomes unsafe. Complete details of this dataset  
88 are provided by Brown and Cote (1992) and the dataset is available on the CIS web site  
89 (<http://www.ec.gc.ca/glaces-ice/>, see Archive followed by Ice Thickness Data). Four sites in the  
90 CAA were selected for study: Alert, Eureka, Resolute, and Cambridge Bay (Figure 1). Although  
91 there are other sites in the database, these sites are the only ones that span the same 55-year  
92 period between 1960 and 2014. The record at Mould Bay, used in BC92, terminated in the early

93 1990s. Together these sites cover  $\sim 20^\circ$  in latitude (Figure 1) that are adjacent to an area of thick  
94 Arctic sea ice that experienced the highest thinning in recent years [*Kwok and Rothrock, 2009*;  
95 *Laxon et al., 2013*]. Values of maximum or end-of-winter ice thickness and corresponding snow  
96 depth during the ice growth season were extracted from the weekly ice and snow thickness data  
97 at the selected sites. As this study is concerned with annual variability in maximum ice thickness,  
98 the main period of interest extends from September to late May.

99 The other source of observed data used in this study were monthly mean air temperature  
100 records at Alert, Eureka, Resolute, and Cambridge Bay for which a complete description is  
101 provided by *Vincent et al. [2012]*.

102

## 103 **2.2. Models**

104 The representation of CAA landfast sea ice thickness within the Coupled Model  
105 Intercomparison project phase 5 (CMIP5) is analyzed using the 1850-2005 Historical experiment  
106 followed by the 2006-2099 Representative Concentration Pathway 8.5 (RCP85) experiment  
107 [*Taylor et al., 2012*] (Table 1). Monthly sea ice thickness (variable *sit*), sea ice concentration  
108 (variable *sic*), 2 meter temperature (variable *tas*) and snow depth (variable *snd*) were used. The  
109 CMIP5 data were retrieved from the British Atmospheric Data Centre database and accessed  
110 through the Center for Environmental Data Analysis ([www.ceda.ac.uk](http://www.ceda.ac.uk)). Ensemble r6i1p1 and  
111 r7i1p1 from model EC-EARTH were removed because of corrupted data. We obtain the multi-  
112 model mean of trends at each grid point by creating the distribution of trends through a Monte-  
113 Carlo simulation. We use a t-distribution for the interannual variability and build a noise model  
114 to account for internal variability as in *Swart et al. [2014]* and *Laliberté et al. [2016]*. The multi-  
115 model mean and its statistical significance is then obtained from the distribution. We obtain the

116 multi-model mean of Pearson correlations by first performing a Fisher transform and then apply  
117 the same method as for the trends. The inverse Fisher transform is applied after obtaining the  
118 multi-model mean and its significance.

119 We also investigate ice thickness values from a selection of the highest resolution models  
120 [Storto *et al.*, 2011; Forget *et al.*, 2015; Haines *et al.*, 2014, Zuo *et al.*, 2015; Masina *et al.*,  
121 2015] from the Ocean Reanalysis Intercomparison (ORA-IP) [Balsameda *et al.*, 2015; Chevallier  
122 *et al.*, 2016] (Table 2) and from the Pan-Arctic Ice-Ocean Modeling and Assimilation System  
123 (PIOMAS) [Zhang and Rothrock, 2003]. Supporting 2 meter temperature data was obtained from  
124 ERA-Interim [Dee *et al.*, 2011].

125

### 126 **3. Results and Discussion: Observations**

#### 127 **3.1. Climatology**

128 The average behavior of landfast ice at the four sites over the 50+ year record is  
129 summarized in Table 3. Ice growth, approximately linear through most of the season, slows after  
130 March (Figure 2). Ice thickness reaches a maximum of ~2-2.3 m by late May at all sites. Values  
131 are consistent with that reported by BC92 and with recent observations of Melling *et al.* [2015]  
132 and Haas and Howell [2015]. The standard deviations are nearly uniform (at ~0.2 m) across all  
133 sites, giving a relatively low coefficient of variation (COV; a measure of relative dispersion  
134 defined as the ratio of the standard deviation to the mean) of ~0.1. The thickest ice is found in  
135 Eureka with a 1957-2014 mean of 2.27 m, which is likely due to climatologically lower air  
136 temperatures in the fall and winter (Table 3).

137 Snow depth also appears to grow linearly through the season, peaking in May but unlike  
138 ice thickness the monthly variability is high (COV ~0.4) (Figure 3). Mean October to May snow

139 depths at Resolute, Eureka and Alert range from ~18-23 cm compared to only ~8 cm at  
140 Cambridge Bay (Table 3). The rapid buildup of the snow cover due to storms in the fall and early  
141 winter that is evident over the Arctic Ocean multi-year ice cover [Warren *et al.*, 1999; Webster *et*  
142 *al.*, 2014], is not seen in these snow depth records within the CAA. The linear behavior in snow  
143 depth is likely maintained by continuous wind-driven redistribution and densification throughout  
144 the ice growth season [BC92; Woo and Heron, 1989].

145

### 146 **3.2. Trends**

147 The time series of maximum ice thickness at Cambridge Bay, Resolute, Eureka and Alert  
148 are illustrated in Figure 4 and summarized in Table 1. Statistically significant (95% or greater  
149 confidence level) negative maximum ice thickness trends are present at Cambridge Bay (-  
150  $4.31 \pm 1.4$  cm decade<sup>-1</sup>), Eureka ( $-4.65 \pm 1.7$  cm decade<sup>-1</sup>) and Alert ( $-4.44 \pm 1.6$  cm decade<sup>-1</sup>) (Table  
151 1). A slight negative trend is present at Resolute but not statistically significant at the 95%  
152 confidence level (Table 1). Over the 50+ year record, the ice thinned by ~0.24-0.26 m at  
153 Cambridge Bay, Eureka and Alert with essentially negligible change at Resolute. These trends in  
154 the CAA are similar to trends on the Siberian coast ( $-3.3$  cm decade<sup>-1</sup>) [Polyakov *et al.*, 2010] but  
155 lower in magnitude compared to the Barents Sea ( $-11$  cm decade<sup>-1</sup>) [Gerland *et al.*, 2008].

156 For the shorter record (late 1950s–1989, ~30 years) investigated by BC92 there was a  
157 negative trend at Alert ( $-7.1$  cm decade<sup>-1</sup>), no evidence of a trend at Eureka, and a positive trend  
158 at Resolute ( $10$  cm decade<sup>-1</sup>) but only the positive trend at Resolute was statistically significant at  
159 the 95% or greater confidence level. Our results from the present 50+ year record suggest that  
160 the negative trend at Alert is robust and the trend at Eureka is now negative and significant. The  
161 trend at Resolute is now slightly negative however it is not statistically significant.

162 Typically, ice thickness reaches its maximum in late May with trends toward earlier dates  
163 of maximum ice thickness present at all sites (significant at Resolute, Eureka and Alert; Table 3).  
164 The significant trends are between  $-2.0 \pm 0.1$  days decade<sup>-1</sup> at Eureka to  $-6.2 \pm 1.5$  days decade<sup>-1</sup> at  
165 Resolute. At Resolute, the date of maximum ice thickness is now on average more than a month  
166 earlier than the early 1960's although this is not reflected in the trend in ice thickness. Freeze  
167 onset at these sites is also increasing at  $\sim 3-6$  days decade<sup>-1</sup> [Howell *et al.*, 2009] and  
168 demonstrates a shortened growth season at Resolute, Eureka and Alert. Together, the trends of  
169 ice thickness and their recorded dates suggest a systematic thinning of landfast ice at Cambridge  
170 Bay, Eureka and Alert.

171

### 172 **3.3. Ice thickness linkages with snow depth and temperature**

173 The variability of landfast thickness at these Arctic sites was previously found to be  
174 largely driven by interannual variations in snow depth and air temperature [BC92; Flato and  
175 Brown, 1996]. With the 50+ year record at the four sites, we can examine the corresponding  
176 linkages to snow depth and temperature.

177 For snow depth, the only trend that is statistically significant at the 95% confidence is  
178 Cambridge Bay at  $-0.8 \pm 0.4$  cm decade<sup>-1</sup> (Table 3). In contrast, BC92 found a significant positive  
179 trend at Alert (4 cm decade<sup>-1</sup>), a trend of low significance in Eureka, and a negative and  
180 significant trend at Resolute ( $-3.3$  cm decade<sup>-1</sup>). Looking at the detrended correlations ( $r$ )  
181 between snow depth and ice thickness reveals the strongest correlation at Resolute ( $r=-0.71$ )  
182 followed by Eureka ( $r=-0.66$ ), Alert ( $r=-0.47$ ) and Cambridge Bay ( $r=-0.31$ ). Figure 6 provides  
183 evidence from extreme years of the role of deeper snow inhibiting ice growth compared to  
184 thinner snow, but the positive trends in snow thickness are not significant at Resolute, Eureka



185 and Alert. This may in part be due to the single pointwise snow depth and ice thickness  
186 measurements made at each point in time, which fail to capture spatial heterogeneity in the snow  
187 depth/ice thickness relationship.

188 With respect to observed temperature, we find significant warming trends in the spring  
189 and fall at all sites over the 50+ year record (Table 3; Figure 7). Significant warming is also  
190 present at all sites in the summer except Resolute and at all sites during the winter except Eureka  
191 (Table 3). Warming is highest during the fall, at  $\sim 0.6^{\circ}\text{C decade}^{-1}$  at all sites (Table 3). The  
192 detrended correlation between temperature (winter, spring, summer and autumn) and maximum  
193 ice thickness is weak at all sites. For example, the strongest detrended correlation between  
194 maximum ice thickness and temperature (winter and spring) is found at Cambridge Bay during  
195 the winter and spring but is only  $\sim 0.4$ .

196 Also of interest is that the observed temperature trends over this period differ  
197 considerably from the earlier period investigated in BC92, in which they reported cooling at all  
198 the sites, with a significant cooling trend at Eureka. It was noted that the general cooling over  
199 their record coincided with the 1946-1986 cooling trend over much of the eastern Arctic and  
200 northwest Atlantic reported by *Jones et al.* [1987]. This cooling trend halted during the 1980s  
201 and the warming, seen in the current and longer record, has resumed [*Jones et al.*, 1999]. Arctic  
202 land areas have experienced an overall warming of about  $\sim 2^{\circ}\text{C}$  since the mid-1960s, with area-  
203 wide positive temperature anomalies that show systematic changes since the end of the 20th  
204 century, which continued through 2014 [*Jeffries and Richter-Menge*, 2015]. Recently, warming  
205 in Canadian Arctic regions was found to be greater than the pan-Arctic trend by up to  $0.2^{\circ}\text{C}$   
206  $\text{decade}^{-1}$  [*Tivy et al.*, 2011].

207

## 208 **4. Results and Discussion: Models**

### 209 **4.1. Climatology**

210 In order to compare seasonal cycles and trends in landfast ice thickness and snow depth  
211 between models and observations, we limit our comparison to models with a reasonable  
212 representation of the CAA, i.e. those with an open Parry Channel (i.e. bcc-csm-1-1, bcc-csm-1-  
213 1m, CNRM-CM5, ACCESS1-0, ACCESS1-3, FIO-ESM, EC-EARTH, inmcm4, MIROC5, MPI-  
214 ESM-LR, MPI-ESM-MR, MRI-CGCM3, CCSM4, NorESM1-M, NorESM1-ME, GFDL-CM3,  
215 GFDL-ESM2G, GFL-ESM2M, CESM1-BCG, CESM1-CAM5, CESM-WACCM). In these  
216 models, sufficient spatial resolution allows us to find sample points that are almost collocated to  
217 *in situ* observation locations. The sample points were determined by finding the closest ocean  
218 grid point where the sea ice is packed for a good portion of the year, but not all year. Grid points  
219 with this characteristic therefore share the most important feature of the landfast ice at our  
220 observations locations: it is not perennial. Mathematically, we sought sample points where the  
221 sea ice concentration is on average above 85% for more than one month but less than 11 months  
222 over the 1955-2014 period. The Eureka site is however particularly challenging for models  
223 because it lies deep in a very narrow channel, which is only resolved by the MPI-ESM-MR in the  
224 CMIP5. As a result, for most models, the sample point for Eureka is located on the western shore  
225 of Ellesmere Island. This is a consequence of using samples as some models either do not  
226 resolve some of the channels in the CAA or have too perennial packed ice cover (e.g. CESM1-  
227 CAM5), then the sample points are further from the observational site than would be desired. We  
228 chose to use sample points in our comparison to observations instead of using regional averages  
229 for two main reasons. The first reason is that using regional averages would have lumped  
230 together different ice dynamics regimes that should not necessarily be expected to compare well

231 to point observations on landfast ice. The second reason is that we are of the opinion that the  
232 resolution in many of these models is sufficiently high to warrant such a direct comparison and  
233 provides a better benchmark than regional averages for landfast ice modelling in the CAA.

234 The seasonal cycle (1955-2014) of median ice thickness from CMIP5 (black), ORA-IP  
235 models CGLORS, ORAP5.0 and GLORYS2V3 (blue), ECCO-v4 (green) and UR025.4 (red) is  
236 shown in Figure 8. ORA-IP models have been split into three groups based, respectively, on their  
237 high, medium and low ice thicknesses at Alert. Ice thickness from CMIP5 is comparable to  
238 observations (Figure 2) at Cambridge Bay and Resolute with maximum ice thickness reaching  
239 200 cm. The ORA-IP models are less consistent. ECCO-v4 tends to have thicker sea ice than  
240 observations at Cambridge Bay, Resolute and Eureka but thinner at Alert. CGLORS, ORAP5.0,  
241 and GLORYS2V3, on the other hand, are comparable to observations at Cambridge Bay,  
242 Resolute and Eureka but have extremely thick and perennial ice close to Alert.

243 The seasonal cycle (1955-2014) of median snow depth from CMIP5 is shown in Figure  
244 9. CMIP5 models indicate a linear increase similar to observations reaching a maximum of ~20  
245 cm in April or May. This is lower than the observed maximum at Resolute, Eureka and Alert but  
246 is about twice as much as at Cambridge Bay. While the snow depth reaches zero during the  
247 summer at Eureka and Alert in models, the sea ice thickness does not (Figure 8), unlike in  
248 observations. This likely reflects the fact that the grid cell thickness in sea ice models with  
249 thickness classes represents the average thickness over these classes. In August the thinner ice  
250 classes might have melted but thicker ice classes can still be found, resulting in a substantial  
251 average ice thickness over the grid cell. The seasonal cycle over packed ice in these models thus  
252 gives a reasonable representation of the seasonal cycle over landfast ice in the CAA, especially  
253 in the southern region of the CAA. Overall, this comparison shows how recent improvements in

254 sea ice model resolution allows comparisons with observations that required dynamical  
255 downscaling techniques in the previous generation of sea ice models [i.e. *Dumas et al. 2005; Sou*  
256 *and Flato, 2013*].

257         Despite relatively high spatial resolution, PIOMAS does not resolve seasonal ice  
258 thickness along the coasts and within the very narrow channels within the CAA (not shown). As  
259 a result, Cambridge Bay and Resolute Bay sites represent the only long-term monitoring sites  
260 within the CAA suitable for comparison since PIOMAS. The monthly time series of PIOMAS  
261 ice and snow thickness estimates at Cambridge Bay and Resolute is shown in Figure 10. The  
262 seasonal cycle of ice growth at Cambridge Bay and Resolute is representative compared to  
263 observations (Figure 2) but PIOMAS estimates retain more ice in August and September,  
264 particularly at Resolute. Ice growth reaches a maximum in April at Cambridge and in May at  
265 Resolute which is 1-month earlier compared to observations. Snow depth follows a linear  
266 increase similar to observations (Figure 3) with good agreement at Cambridge Bay but  
267 considerably underestimates snow depth at Resolute (Figure 10). *Schweiger et al.* [2011]  
268 performed a detailed comparison of PIOMAS ice thickness values against *in situ* and Ice, Cloud,  
269 and land Elevation Satellite (ICESat) ice thickness observations and found strong correlations.  
270 They determined a root mean square error (RMSE) of ~0.76 m and noted that PIOMAS  
271 generally overestimates thinner ice and underestimates thicker ice. At both sites within the CAA,  
272 PIOMAS ice thickness data is in reasonably good agreement with *in situ* observations with  
273 RMSE's of 0.29 cm at Cambridge Bay and 0.68 cm at Resolute (Figure 11). The systematic  
274 overestimate of thinner ice reported by *Schweiger et al.* [2011] is more apparent at Resolute than  
275 Cambridge Bay (Figure 11). The higher latitude regions of the CAA where there is an intricate

276 mix of seasonal first-year ice and multi-year ice is a problem for PIOMAS and thus contributes  
277 to the larger discrepancy at Resolute compared to Cambridge Bay.

278

## 279 **4.2. Trends**

280 The spatial distribution of maximum sea ice thickness trends from ORA-IP and CMIP5 is  
281 illustrated in Figures 12. The CMIP5 model-mean exhibit a fairly uniform trend pattern,  
282 consistent with the different in situ observations (Figure 4) but with overestimated negative  
283 thickness trends. Although, for individual models this pattern is far from uniform, the general  
284 pattern and magnitude of thickness trends tend to be roughly in accordance with temperature  
285 trends (not shown). A similar behavior is observed in the ORA-IP models, with the notable  
286 exception of CGLORS, where positive thickness trends are found almost everywhere (Figure  
287 12a). This is robust and it appears that the model is not completely equilibrated in the CAA and  
288 exhibit large month-to-month adjustments. Model ORAP5.0 also is not completely equilibrated  
289 in the region for years 1979-1984. During those years, it exhibits large inter annual changes in  
290 thickness. For this reason, we are only considering years 1985-2013 for this model.

291 For PIOMAS, the North-South overestimated trend is also present (not shown) as with  
292 CMIP5 and ORA-IP. Looking specifically at trends computed from 1979-2014 near the observed  
293 sites indicates that the mean maximum ice thickness linear trend from at Cambridge Bay is -  
294  $13.4 \pm 3.4$  cm decade<sup>-1</sup> which is almost double the observational trend of  $6.2 \pm 2.4$  cm decade<sup>-1</sup>. At  
295 Resolute, the PIOMAS linear trend is  $24.0 \pm 4.1$  cm decade<sup>-1</sup> which is considerably stronger than  
296 the observational trend of  $-4.9 \pm 3.51$  cm decade<sup>-1</sup>.

297

## 298 **4.3. Ice thickness linkages with snow depth and temperature**

299 Even though ORA-IP models have unrealistically large thickness trends, the pattern of  
300 inter annual correlation (detrended) between winter temperatures and thicknesses is roughly  
301 consistent across models (Figure 13). Some ORA-IP models also experience positive correlations  
302 (e.g. CGLORS, ORAP5.0, GLORYS2V3 and UR025.4) that are mostly located north of the  
303 CAA or within the CAA in regions where multi-year ice is known to be present. It is possible  
304 that warmer temperatures are associated with an increased flux of thicker multi-year ice into the  
305 CAA which is known to occur [e.g. *Howell et al.*, 2013] but the driving processes responsible for  
306 these positive correlations require more investigation. In CMIP5 models, no model exhibits  
307 positive correlations with temperature that resemble ORA-IP models over the CAA. Although  
308 the time series for the ORA-IP models is short and the positive correlations are only statistically  
309 significant at a few grid points in CGLORS and UR025.4, this behavior is sufficiently  
310 problematic to recommend that care should be taken when using these ORA-IP models to study  
311 the interannual variability in the Canadian Arctic.

312 In the CMIP5 models, significant winter snow depth trends are more strongly negative in  
313 the North than in the South (Figure 14). This is in disagreement with point observations  
314 presented in the previous sections that showed no significant trends snow depth trends at Alert  
315 but negative and significant trends at Cambridge Bay. Although only based on limited point *in*  
316 *situ* observations, this suggests that over the last decades changes in winter precipitation at Alert  
317 must have compensated the increased melting driven by increasing temperatures, a compensation  
318 that is clearly not captured in CMIP5 models..

319

## 320 **5. Conclusions**

321 Over the 50+ year in situ observational record, statistically significant negative trends in  
322 maximum (end-of-winter) ice thickness are present at Cambridge Bay, Eureka and Alert.  
323 Significant negative trends in the day of maximum ice thickness are also present at Resolute,  
324 Eureka and Alert. Together, these trends suggest thinning of landfast ice in the CAA, where little  
325 evidence was found in the shorter record analyzed in an earlier study (BC92). The inter-annual  
326 variability of air temperature is only weakly correlated to maximum ice thickness (i.e. maximum  
327 correlation is ~0.4). Snow thickness plays the dominant role in controlling maximum ice  
328 thickness variability given the high correlations at Resolute and Eureka and reasonably high  
329 correlations at Alert and Cambridge Bay.

330 Comparison of CMIP5, ORA-IP and PIOMAS simulations with observations indicate a  
331 reasonable representation of the landfast ice thickness monthly climatology within the CAA.  
332 This is particularly apparent when seasonal first-year ice dominates the icescape (i.e. Cambridge  
333 Bay). Despite improvements in spatial resolution, mixed ice types (i.e. seasonal and multi-year)  
334 present at the sub-grid cell resolution are likely problems for model estimates within the CAA.  
335 The overall thickness of ice within the CAA in the current generation of models is too high. As a  
336 result, trends are unrealistic and far exceed observations (by upwards of  $-50 \text{ cm decade}^{-1}$ ) in part  
337 because the initial ice thickness is too large. The problem is particularly acute in the ORA-IP  
338 models where large and unrealistic inter annual changes in thickness suggest that the models are  
339 not fully equilibrated.

340 While the impact of the snow cover on ice thickness is well known, the significant  
341 correlations at Resolute, Eureka and Alert suggest that the higher sensitivity to changes in snow  
342 depth could potentially mask the warming signal on both fast and offshore ice. Thus, even in this  
343 limited data set, we can see the dominant role played by snow depth in determining the

344 interannual variability of the maximum landfast ice thickness. This again highlights that the  
345 primary factor is the amount and timing of snow accumulation, not air temperature. However, it  
346 is worth noting that few of the current generation models show coherent relationships between  
347 ice thickness, snow depth and temperature over the longer term record.

348

#### 349 **Authors Contributions**

350 S.E.L.H, F.L and R.K designed the study, performed the analysis and wrote the manuscript with  
351 input from C.D. and J.K.

352

#### 353 **Acknowledgements**

354 The authors wish to thank all the individuals responsible for collecting landfast ice and snow  
355 thickness measurements in the Canadian Arctic over the past 50+ years.

356

357

#### 358 **References**

359

360 Alt, B., K. Wilson, and T. Carrieres (2006), A case study of old ice import and export through  
361 Peary and Sverdrup channels in the Canadian Arctic Archipelago: 1998-2004, *Ann. Glaciol.*, 44,  
362 329–338, doi:10.3189/172756406781811321.

363

364 M.A. Balmaseda , F. Hernandez , A. Storto , M.D. Palmer , O. Alves , L. Shi , G.C. Smith , T.  
365 Toyoda , M. Valdivieso , B. Barnier , D. Behringer , T. Boyer , Y-S. Chang , G.A. Chepurin , N.  
366 Ferry , G. Forget , Y. Fujii , S. Good , S. Guinehut , K. Haines , Y. Ishikawa , S. Keeley , A.  
367 Köhl , T. Lee , M.J. Martin , S. Masina , S. Masuda , B. Meyssignac , K. Mogensen , L. Parent ,  
368 K.A. Peterson , Y.M. Tang , Y. Yin , G. Vernieres , X. Wang , J. Waters , R. Wedd , O. Wang ,  
369 Y. Xue , M. Chevallier , J-F. Lemieux , F. Dupont , T. Kuragano , M. Kamachi , T. Awaji , A.  
370 Caltabiano , K. Wilmer-Becker , F. Gaillard, The Ocean Reanalyses Intercomparison Project  
371 (ORA-IP), *Journal of Operational Oceanography*, Vol. 8, Iss. sup1, 2015,  
372 DOI:10.1080/1755876X.2015.1022329

373

374 Brown, R., and P. Cote (1992), Interannual variability of landfast ice thickness in the Canadian  
375 high arctic, 1950–89. *Arctic*, 45, 273–284.

376



377 Bromwich, D. H., A. B. Wilson, L. Bai, G. W. K. Moore, and P. Bauer, 2015: A comparison of  
378 the regional Arctic System Reanalysis and the global ERA-Interim Reanalysis for the Arctic. *Q.*  
379 *J. R. Meteorol. Soc.*, doi: 10.1002/qj.2527  
380

381 Dee DP, co-authors (2011), The ERA-Interim reanalysis: configuration and performance of the  
382 data assimilation system. *Q J R Meteorol Soc.* 137: 553–597, doi:10.1002/qj.828.  
383

384 Dumas, J. A., G. M. Flato, and R. D. Brown (2006), Future projections of landfast ice thickness  
385 and duration in the Canadian Arctic. *J. Climate*, 19, 5175–5189.  
386

387 Druckenmiller, M. L., H. Eicken, M. A. Johnson, D. J. Pringle, and C. C. Williams (2009),  
388 Toward an integrated coastal sea-ice observatory: System components and a case study at  
389 Barrow, Alaska. *Cold Reg.Sci.Tech.*, 56, 61-72.  
390

391 Flato, G. M., and R. D. Brown (1996), Variability and climate sensitivity of landfast Arctic sea  
392 ice. *J. Geophys. Res.*, 101 (C10), 25 767–25 777.  
393

394 Forget, G., Campin, J.-M., Heimbach, P., Hill, C. N., Ponte, R. M., and Wunsch, C. (2015),  
395 ECCO version 4: an integrated framework for non-linear inverse modeling and global ocean  
396 state estimation, *Geosci. Model Dev.*, 8, 3071-3104, doi:10.5194/gmd-8-3071-2015/  
397

398 Gerland, S., A. H. H. Renner, F. Godtliessen, D. Divine, and T. B. Loynning (2008), Decrease of  
399 sea ice thickness at Hopen, Barents Sea, during 1966-2007. *Geophys. Res. Lett.*, 35, L06501.  
400

401 Gough, W., A.S. Gagnon and H.P Lau (2004), Interannual variability of Hudson Bay Ice  
402 Thickness, *Polar Geography*, 28(3), 222-238.  
403

404 Haines K, M. Valdivieso, H. Zuo, and V.N. Stepanov (2012), Transports and budgets in a 1/4 °  
405 global ocean reanalysis 1989–2010. *Ocean Sci.* 8(3): 333–344, doi:10.5194/os-8-333-  
406 2012.002/qj.2063.  
407

408 Haas, C., and S. E. L. Howell (2015), Ice thickness in the Northwest Passage, *Geophys. Res.*  
409 *Lett.*, 42, doi:10.1002/2015GL065704  
410

411 Howell, S. E. L., C. R. Duguay, and T. Markus (2009), Sea ice conditions and melt season  
412 duration variability within the Canadian Arctic Archipelago: 1979–2008, *Geophys. Res. Lett.*,  
413 36, L10502, doi:10.1029/2009GL037681.

414 Howell, S. E. L., T. Wohlleben, M. Daboor, C. Derksen, A. Komarov, and L. Pizzolato (2013),  
415 Recent changes in the exchange of sea ice between the Arctic Ocean and the Canadian Arctic  
416 Archipelago, *J. Geophys. Res. Oceans*, 118, 3595–3607, doi:10.1002/jgrc.20265.

417 Jeffers, S., T. Agnew, B. Alt, R. De Abreu, and S. McCourt (2001), Investigating the anomalous  
418 sea ice conditions in the Canadian High Arctic (Queen Elizabeth Islands) during the summer of  
419 1998, *Ann. Glaciol.*, 33, 507– 612.  
420

421 Jeffries, M. O. and J. Richter-Menge, Eds. (2015), The Arctic [in State of the Climate in 2014],  
422 *Bull. Amer. Meteor. Soc.*, 96, ES1–ES32.

423 doi: <http://dx.doi.org/10.1175/2015BAMSStateoftheClimate.1>  
424  
425 Jones, P.D., T.M.L. Wigley, C.K. Folland and D.E. Parker (1987), Spatial patterns in recent  
426 worldwide temperature trends. *Climate Monitor*, 16(5): 175-185.  
427  
428 Jones, P.D., M. New, D.E. Parker, S. Martin, and I.G. Rigor (1999), Surface air temperature and  
429 its changes over the past 150 years, *Rev. Geophys.*, 37(2),173–200.  
430  
431 Kwok, R., and D. A. Rothrock (2009), Decline in Arctic sea ice thickness from submarine and  
432 ICESat records: 1958 – 2008, *Geophys. Res. Lett.*, 36, L15501, doi:10.1029/2009GL039035.  
433  
434 Laliberté, F., S. E. L. Howell, and P. J. Kushner (2016), Regional variability of a projected sea  
435 ice-free Arctic during the summer months, *Geophys. Res. Lett.*, 43, 256–263,  
436 doi:10.1002/2015GL066855.  
437  
438 Laxon S. W., K. A. Giles, A. L. Ridout, D. J. Wingham, R. Willatt, R. Cullen, R. Kwok, A.  
439 Schweiger, J. Zhang, C. Haas, S. Hendricks, R. Krishfield, N. Kurtz, S. Farrell and M. Davidson  
440 (2013), CryoSat-2 estimates of Arctic sea ice thickness and volume, *Geophys. Res. Lett.*, 40,  
441 732–737, doi:10.1002/grl.50193.  
442  
443 Masina, S. et al. (2015), An ensemble of eddy-permitting global ocean reanalyses from the  
444 MyOcean project. *Clim. Dynam.* 1–29, doi:10.1007/s00382-015-2728-5  
445  
446 Mahoney, A., H. Eicken, and L. Shapiro (2007), How fast is landfast sea ice? A study of the  
447 attachment and detachment of nearshore ice at Barrow, Alaska. *Cold Reg.Sci.Tech.*, 47, 233-255.  
448  
449 Mahoney, A. R., H. Eicken, A. G. Gaylord, and R. Gens (2014), Landfast sea ice extent in the  
450 Chukchi and Beaufort seas: The annual cycle and decadal variability, *Cold Reg. Sci. Technol.* ,  
451 103, 41–56, doi:10.1016/j.coldregions.2014.03.003.  
452  
453 Melling, H. (2002), Sea ice of the northern Canadian Arctic Archipelago, *J. Geophys. Res.*,  
454 107(C11), 3181, doi:10.1029/2001JC001102.  
455  
456 Melling, H., C. Haas, and E. Brossier (2015), Invisible polynyas: Modulation of fast ice  
457 thickness by ocean heat flux on the Canadian polar shelf, *J. Geophys. Res. Oceans*, 120, 777–  
458 795, doi:10.1002/2014JC010404.  
459  
460 Ólason, E. Ö. (2012), Dynamical modeling of Kara Sea land-fast ice, PhD thesis, Univ. of  
461 Hamburg, Hamburg, Germany.  
462  
463 Polyakov, I. V., et al. (2010), Arctic Ocean Warming Contributes to Reduced Polar Ice Cap.  
464 *Journal of Physical Oceanography*, 40, 2743-2756  
465  
466 Schweiger, A., R. Lindsay, J. Zhang, M. Steele, H. Stern, and R. Kwok (2011), Uncertainty in  
modeled Arctic sea ice volume, *J. Geophys. Res.*, 116, C00D06, doi:10.1029/2011JC007084.

467 Serson, H.V. (1972), Investigations of a plug of multiyear old sea ice in the mouth of Nansen  
468 Sound. Ottawa, Ont., Department of National Defence, Canada. Defence Research Establishment  
469 Ottawa. (DREO Tech. Note 72-6.)  
470

471 Serson, H.V. (1974), Sverdrup Channel. Ottawa, Ont., Department of National Defence, Canada.  
472 Defence Research Establishment Ottawa. (DREO Tech. Note 74-10.)  
473

474 Sou, T., and G. Flato (2009), Sea ice in the Canadian Arctic Archipelago: Modeling the past  
475 (1950-2004) and the future (2041-60), *J. Clim.*, 22, 2181–2198, doi:10.1175/2008JCLI2335.1  
476 Stroeve, J. C., M. C. Serreze, M. M. Holland, J. E. Kay, J. Malanik, and A. P. Barrett (2011),  
477 The Arctic's rapidly shrinking sea ice cover: A research synthesis, *Clim. Change*, 110(3-4),  
478 1005–1027.  
479

480 Storto A, S. Dobricic S, S. Masina and D. Di Pietro (2011), Assimilating along-track altimetric  
481 observations through local hydrostatic adjustments in a global ocean reanalysis system. *Mon*  
482 *Wea Rev.* 139: 738–754.  
483

484 Stroeve, J. C., M. C. Serreze, M. M. Holland, J. E. Kay, J. Maslanik, and A. P. Barrett (2012),  
485 The Arctic's rapidly shrinking sea ice cover: A research synthesis, *Clim. Change*, 110(3–4),  
486 1005–1027

487 Swart, N. C., J. C. Fyfe, E. Hawkins, J. E. Kay, and A. Jahn (2015), Influence of internal  
488 variability on Arctic sea-ice trends, *Nat. Clim. Change*, 5, 86–89, doi:10.1038/nclimate2483.  
489

490 Taylor, K. E., R. J. Stouffer, and G. A. Meehl (2012), An overview of CMIP5 and the  
491 experiment design, *Bull. Am. Meteorol. Soc.*, 93, 485–498, doi:10.1175/BAMS-D-11-00094.1.  
492

493 Tivy, A., S. E. L. Howell, B. Alt, S. McCourt, R. Chagnon, G. Crocker, T. Carrieres, and J. J.  
494 Yackel (2011), Trends and variability in summer sea ice cover in the Canadian Arctic based on  
495 the Canadian Ice Service Digital Archive, 1960–2008 and 1968–2008, *J. Geophys. Res.*, 116,  
496 C03007, doi:10.1029/2009JC005855.  
497

498 Vincent, L., X. Wang, E. Milewska, Hui Wan, F. Yang, and V. Swail (2012), A second  
499 generation of homogenized Canadian monthly surface air temperature for climate trend analysis.  
500 *Journal of Geophysical Research*, D18110, doi:10.1029/2012JD017859  
501

502 Warren, S. G., I. G. Rigor, N. Untersteiner, V. F. Radionov, N. N. Bryazgin, Y. I. Aleksandrov,  
503 and R. Colony (1999), Snow depth on Arctic sea ice, *J. Clim.*, 12, 1814–1829.  
504

505 Wilks, D. S. (2006). On “field significance” and the false discovery rate. *J. Appl. Meteor.*  
506 *Climatol.*, 45, 1181–1189. doi: <http://dx.doi.org/10.1175/JAM2404.1>  
507 Woo, M-K., and R. Heron (1989), Freeze-up and break-up of ice cover on small arctic lakes. In:  
508 Mackay, W.C., ed. Northern lakes and rivers. Edmonton: Boreal Institute for Northern Studies,  
509 56-62.  
510

511 Woo, M-K., R. Heron, P. Marsh, and P. Steer, (1983), Comparison of weather station snowfall  
512 with winter snow accumulation in High Arctic basins, *Atmos.-Ocean*, 21(3):312-325.

513  
514 World Meteorological Organization, (1970), WMO sea-ice nomenclature. Terminology, codes  
515 and illustrated glossary. WMO/OMM.BMO No. 259, 145 pp, Geneva Secretariat of the World  
516 Meteorological Organization  
517  
518 Yu, Y, H. Stern, C. Fowler, F. Fetterer, and J. Maslanik (2014), Interannual Variability of Arctic  
519 Landfast Ice between 1976 and 2007. *J. Climate*, **27**, 227–243.  
520 doi: <http://dx.doi.org/10.1175/JCLI-D-13-00178.1>  
521  
522 Zhang, J.L. and D.A. Rothrock, (2003), Modeling global sea ice with a thickness and enthalpy  
523 distribution model in generalized curvilinear coordinates, *Mon. Weather Rev.*, 131, 845-861.  
524 Zuo, H., M.A. Balmaseda, and K. Mogensen (2015), The new eddy-permitting ORAP5 ocean  
525 reanalysis: description, evaluation and uncertainties in climate signals. *Clim. Dynam.* 1–21.  
526 doi:10.1007/s00382-015-2675-1.  
527  
528  
529  
530  
531  
532  
533  
534  
535  
536  
537  
538  
539  
540  
541  
542  
543  
544  
545  
546  
547  
548  
549  
550  
551  
552  
553  
554  
555  
556  
557 Table 1. CMIP5 models used in this study, the number of realizations with ice data and the  
558 number of realizations with sea ice transport data

	w/ ice		w/ ice
bcc-csm1-1	1	MIROC-ESM-CHEM	1
bcc-csm1-1-m	1	MIROC5	3
BNU-ESM	1	HadGEM2-CC	1
CanESM2	5	HadGEM2-ES	4
CMCC-CESM	1	MPI-ESM-LR	3
CMCC-CM	1	MPI-ESM-MR	1
CMCC-CMS	1	MRI-CGCM3	1
CNRM-CM5	5	CCSM4	6
ACCESS1.0	1	NorESM1-M	1
ACCESS1.3	1	NorESM1-ME	1
CSIRO-Mk3.6.0	10	GFDL-CM3	1
FIO-ESM	1	GFDL-ESM2G	1
EC-EARTH	6	GFDL-ESM2M	1
inmcm4	1	CESM1(BGC)	1
FGOALS-g2	1	CESM1(CAM5)	3
MIROC-ESM	1	CESM1(WACCM)	3

559  
560  
561  
562  
563  
564  
565  
566  
567  
568  
569  
570  
571  
572  
573  
574  
575  
576  
577  
578  
579

580 Table 2. Summary of ORA-IP models characteristics

<b>Model Name</b>	<b>CGLORS</b>	<b>ECCO-v4</b>	<b>GLORYS2V3</b>	<b>ORAP5.0</b>	<b>UR025.4</b>	<b>PIOMASS</b>
<b>Institute</b>	CMCC	JPL-NASA-MIT-AER	Mercator Océan	ECMWF	University of Reading	APL/PSC
<b>Resolution</b>	ORCA0.25°	~40km in the Arctic	ORCA0.25°	ORCA0.25°	ORCA0.25°	~22km in the Arctic
<b>Ocean Model</b>	NEMO 3.2.1	MITgcm	NEMO 3.1	NEMO3.4	NEMO 3.2	POP
<b>Sea ice Model</b>	LIM2	MITgcm	LIM2 (with EVP rheology)	LIM2	LIM2	TED
<b>Time period considered</b>	1982-2012	1991-2011	1993-2013	1985-2013	1993-2010	1958-2015
<b>Atmospheric forcing</b>	ERA-Interim	ERA-Interim	ERA-Interim	ERA-Interim	ERA-Interim	NCEP/NCAR
<b>Sea ice product assimilated</b>	NSIDC NASA-Team Daily	NSIDC Bootstrap Monthly	IFREMER/CERSAT	NOAA / OSTIA combination	EUMETSAT OSI-SAF	NSIDC near-real time Daily

581  
582  
583  
584  
585  
586  
587  
588  
589  
590  
591  
592  
593  
594  
595  
596  
597  
598  
599  
600  
601  
602  
603  
604  
605

606 Table 3. Observed maximum ice thickness, snow depth, and surface air temperature at four  
 607 landfast ice sites in the Canadian Arctic Archipelago. The bold text indicates statistical  
 608 significance of the linear trend at 95% or greater.

	Cambridge Bay	Resolute	Eureka	Alert
Period	1960-2014	1957-2014	1957-2014	1957-2014
Ice Thickness, $h_{ice}$				
Mean of $max h_{ice}$ (m)	2.11±0.19	2.02±0.19	2.27±0.23	1.98±0.22
Trend of $max h_{ice}$ (cm decade <sup>-1</sup> )	<b>-4.31±1.4</b>	-0.5±1.6	<b>-4.65±1.7</b>	<b>-4.44±1.6</b>
Day of $max h_{ice}$	24 May±17	25 May±21	26 May±12	27 May±16
Trend of day of $max h_{ice}$ (days decade <sup>-1</sup> )	-0.87±1.5	<b>-6.2±1.5</b>	<b>-2.0±0.1</b>	<b>-3.0±1.2</b>
Snow depth ( $h_{snow}$ )				
Mean Oct-May $h_{snow}$ (cm)	8.4±4.2	22.6±10	17.6±5.8	18.4±6.2
Trend of Oct-May $h_{snow}$ (cm decade <sup>-1</sup> )	<b>-0.8±0.4</b>	-0.75±0.8	0.54±0.5	0.26±0.5
Temperature				
Winter (Dec-Feb) Mean (°C)	-31.3±2.0	-30.8±1.9	-36.0±2.0	-31.2±1.6
Winter (Dec-Feb) (°C/decade)	<b>0.59±0.2</b>	<b>0.35±0.1</b>	0.23±0.2	<b>0.38±0.1</b>
Spring (Mar-May) Mean (°C)	-20.0±1.8	-21.1±1.8	-24.9±2.0	-22.8±1.8
Spring (Mar-May) (°C/decade)	<b>0.47±0.1</b>	<b>0.57±0.1</b>	<b>0.44±0.1</b>	<b>0.32±0.1</b>
Summer (Jun-Aug) Mean (°C)	5.9±1.4	2.3±1.3	3.9±1.2	1.3±0.8
Summer (Jun-Aug) (°C/decade)	<b>0.30±0.1</b>	0.17±0.2	<b>0.21±0.1</b>	<b>0.1±0.1</b>
Fall (Sep-Nov) Mean (°C)	-11.1±2.0	-13.8±2.0	-19.6±2.2	-18.0±1.7
Fall (Sep-Nov) (°C/decade)	<b>0.60±0.2</b>	<b>0.67±0.1</b>	<b>0.68±0.2</b>	<b>0.56±0.1</b>

609  
 610  
 611  
 612  
 613  
 614

615 **List of Figures**

616

617 Figure 1. Map of the central Canadian Arctic Archipelago showing the location of the landfast  
618 snow and thickness observations.

619

620 Figure 2. Seasonal cycle of observed mean ice thickness at the four sites (1960-2014).

621

622 Figure 3. Seasonal cycle of observed mean snow depth at the four sites (1960-2014).

623

624 Figure 4. Time series and trend of observed maximum ice thickness at the four sites.

625

626 Figure 5. Time series and trend of observed mean October through May snow depth at the four  
627 sites.

628

629 Figure 6. Weekly time series of ice thickness and snow depth at Eureka and Alert for (a) low  
630 snow years and (b) high snow years.

631

632 Figure 7. Time series of mean air temperature during winter (DJF), spring, (MAM), summer  
633 (JJA) and autumn (SON) at the four sites.

634

635 Figure 8. CMIP5 median sea ice thickness seasonal cycle (1955-2014) at stations (grey).  
636 Observations from 2 (black). Median of ORA-IP models CGLORS, ORAP5.0, GLORYS2V3  
637 (blue), ECCO-v4 (green) and UR025.4 (red). Whiskers indicate the 5th and 95th percentiles.

638

639 Figure 9. Same as Figure 8 for snow depth and only for CMIP5 models (grey) and observations  
640 (black).

641

642 Figure 10. Seasonal cycle of observed mean ice thickness (left) and snow depth (right) from  
643 PIOMAS at Cambridge Bay and Resolute (1979-2014).

644

645 Figure 11. Comparison of PIOMAS ice thickness with ice thickness observations from  
646 Environment Canada's ice thickness monitoring sites at Cambridge Bay and Resolute. The data  
647 covers the period 1979-2014.

648

649 Figure 12. **a-e:** Maximum sea ice thickness trends in ORA-IP simulations. **f:** Same for CMIP5  
650 MODEL-MEAN. From South to North, o's indicate Cambridge Bay (green), Resolute (blue),  
651 Eureka (white) and Alert (black) and x's indicate the corresponding measurement stations. In **f**,  
652 one o per model is shown." The stippling indicates p-values less than 0.05, corrected using the  
653 False Discovery Rate (FDR) method with a global pFDR-values less than 0.10 [Wilks, 2006].  
654 The colorbar is linear from -10 cm dec-1 to 10 cm dec-1 and symmetric logarithmic beyond  
655 these values.

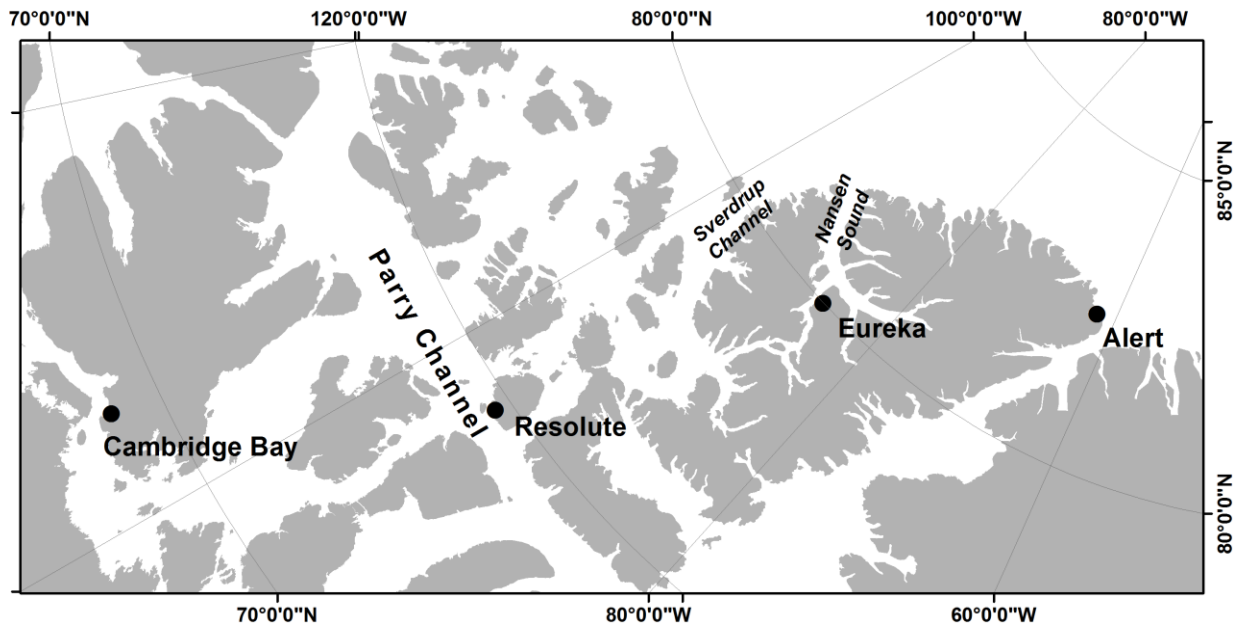
656

657 Figure 13. **a-e:** Pearson correlation of detrended maximum sea ice thickness in ORA-IP with  
658 detrended ONDJFMAM ERA-INTERIM 2m temperature. **f:** Same but for CMIP5 MODEL-  
659 MEAN. The stippling indicates p-values less than 0.05, corrected using the False Discovery Rate  
660 (FDR) method with a global pFDR-values less than 0.10 [Wilks, 2006].



661  
662  
663  
664  
665  
666  
667  
668  
669  
670  
671  
672  
673  
674  
675  
676  
677  
678  
679  
680  
681  
682  
683  
684  
685  
686  
687  
688  
689  
690  
691  
692  
693  
694  
695  
696  
697  
698  
699  
700  
701

Figure 14. Same as Figure 12f but for snow depth trends (ONDFJMAM).



702  
 703  
 704  
 705  
 706  
 707  
 708  
 709

Figure 1. Map of the central Canadian Arctic Archipelago showing the location of the landfast snow and thickness observations.

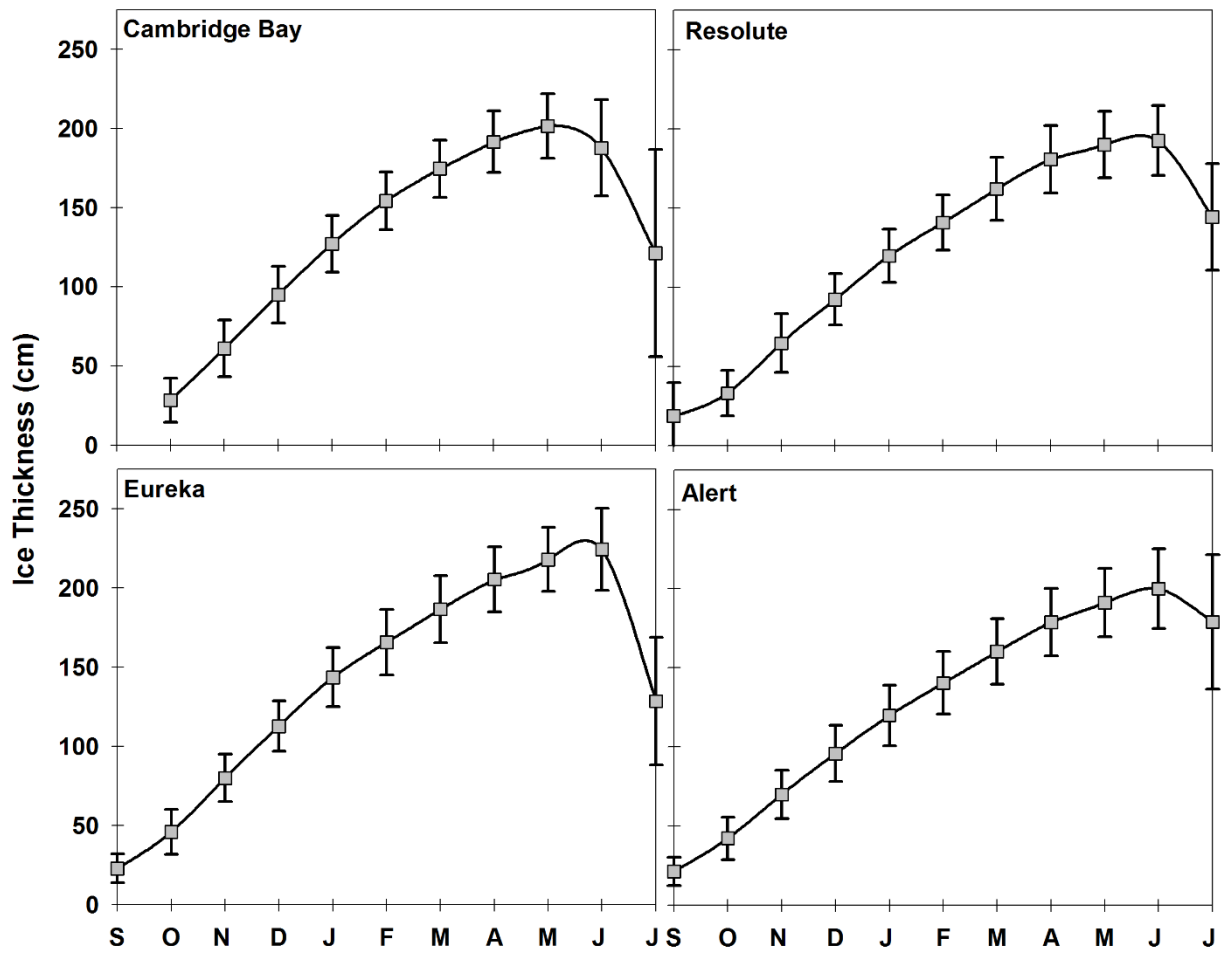


Figure 2. Seasonal cycle of observed mean ice thickness at the four sites (1960-2014).

710  
 711  
 712  
 713  
 714  
 715  
 716  
 717  
 718  
 719  
 720

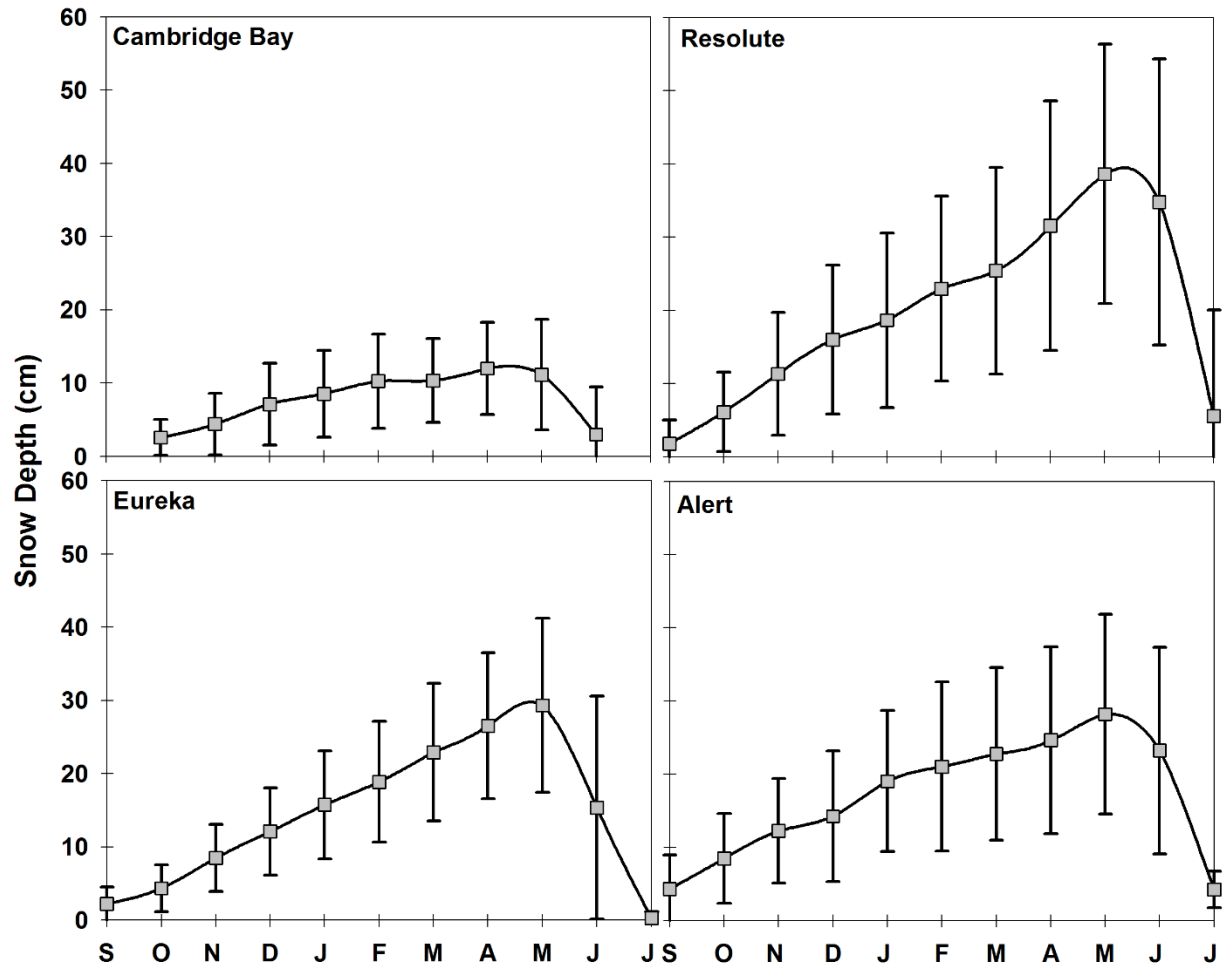


Figure 3. Seasonal cycle of observed mean snow depth at the four sites (1960-2014).

721  
 722  
 723  
 724  
 725  
 726  
 727

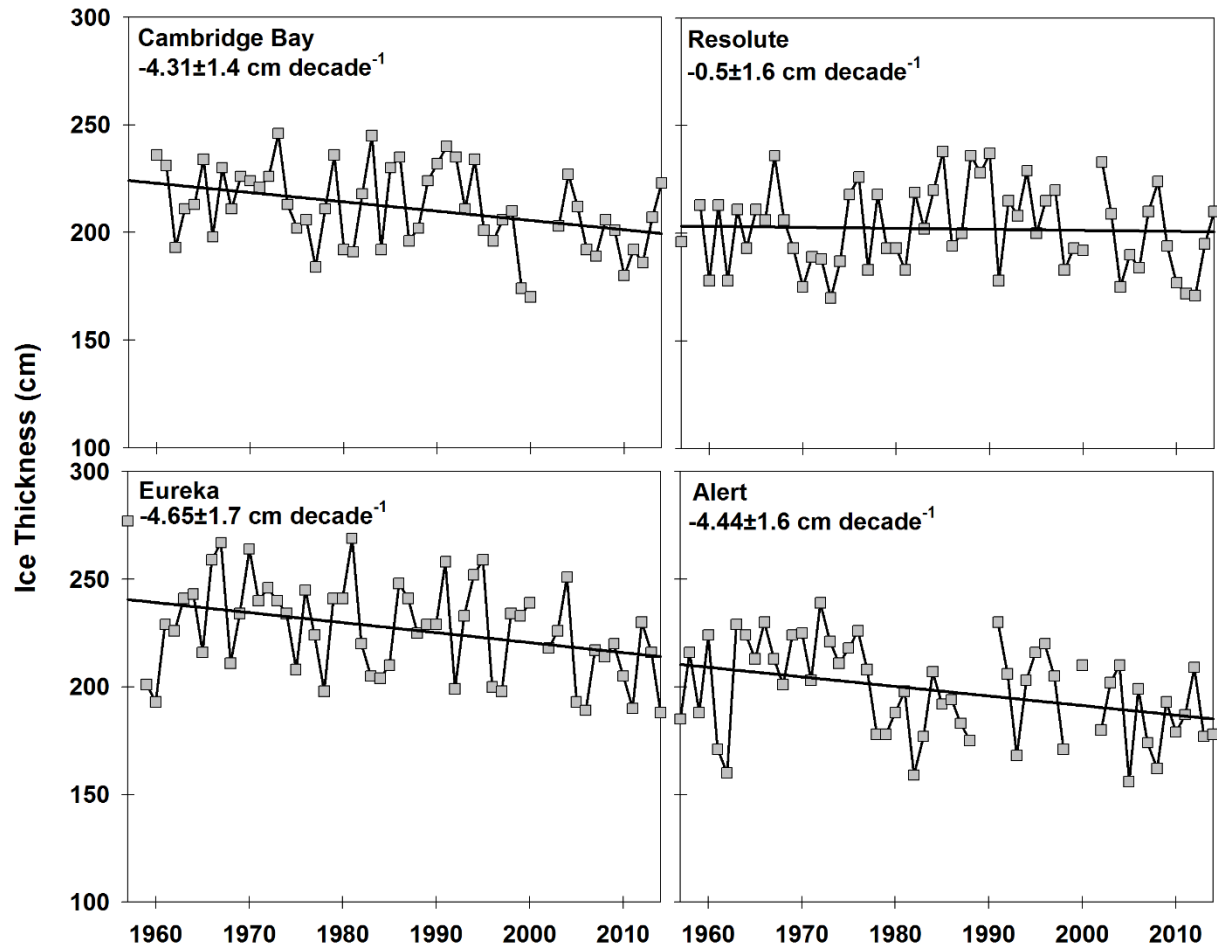
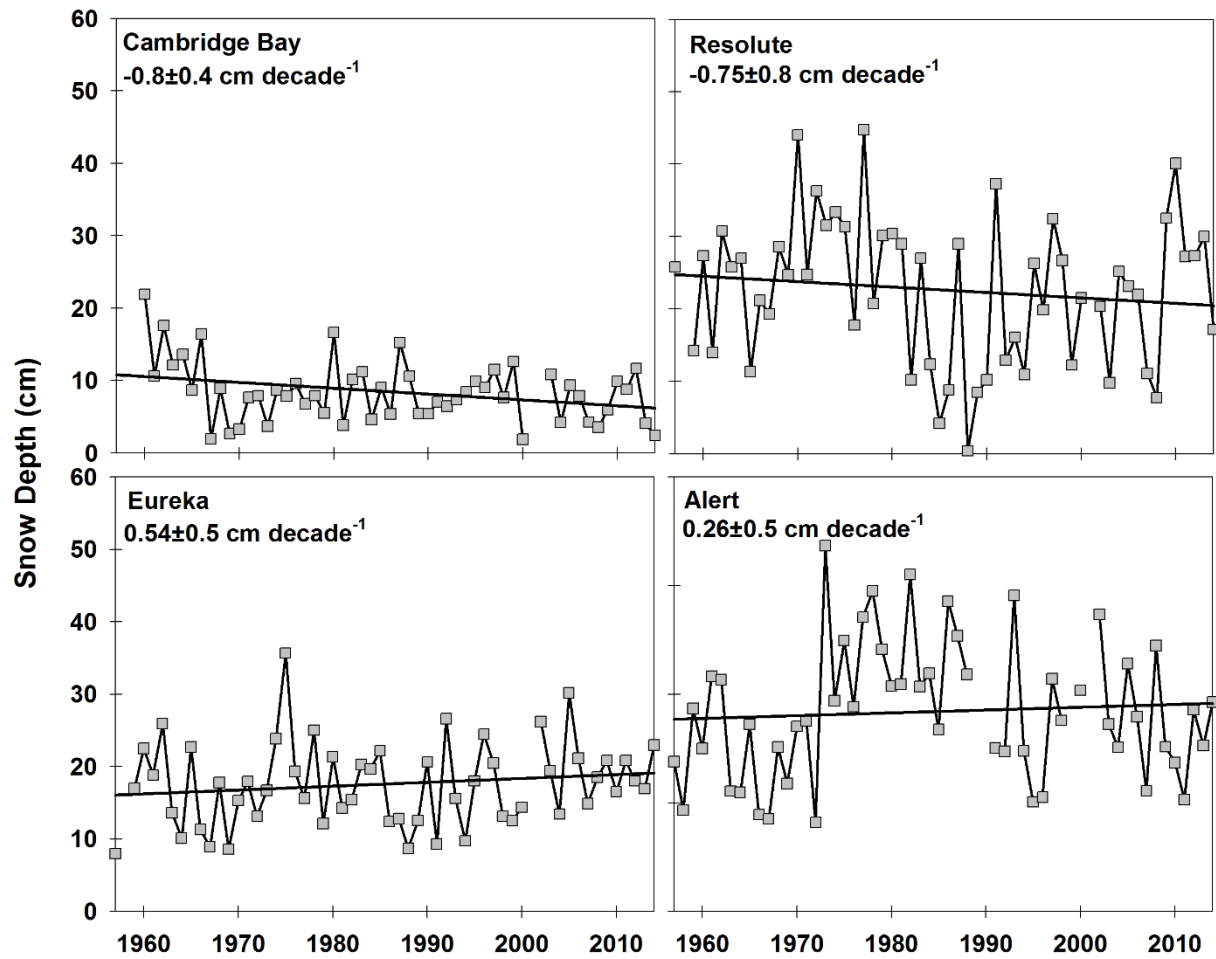


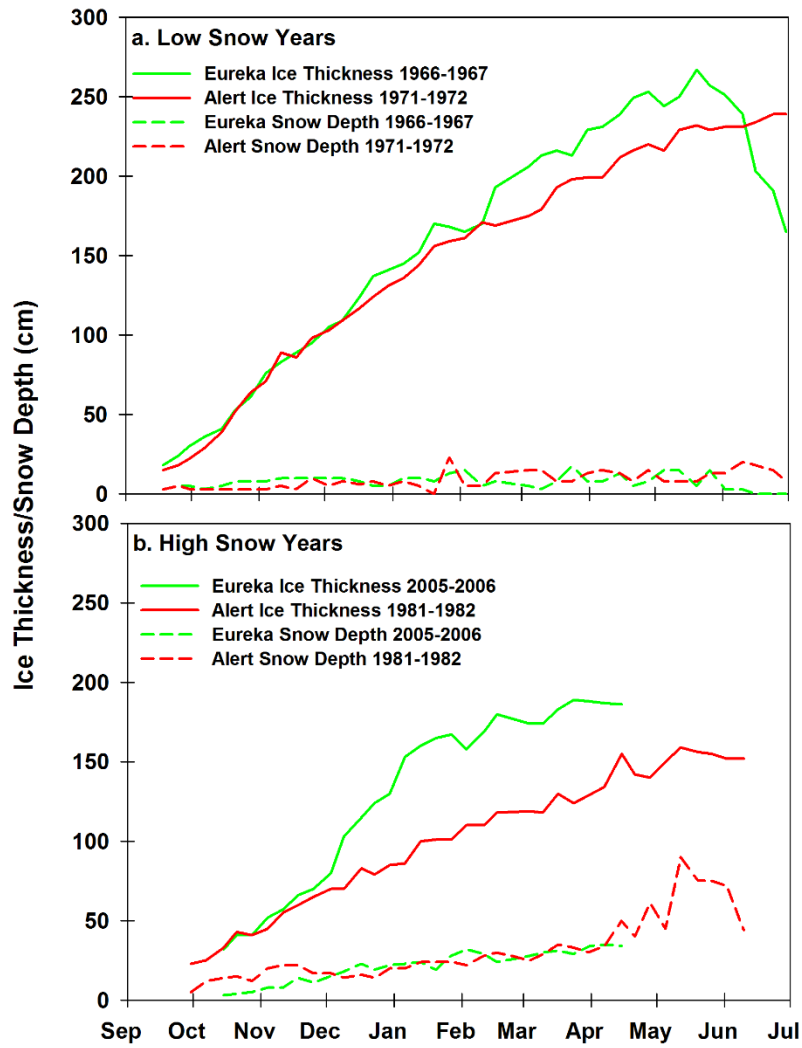
Figure 4. Time series and trend of observed maximum ice thickness at the four sites.

728  
 729  
 730  
 731  
 732  
 733  
 734  
 735  
 736  
 737



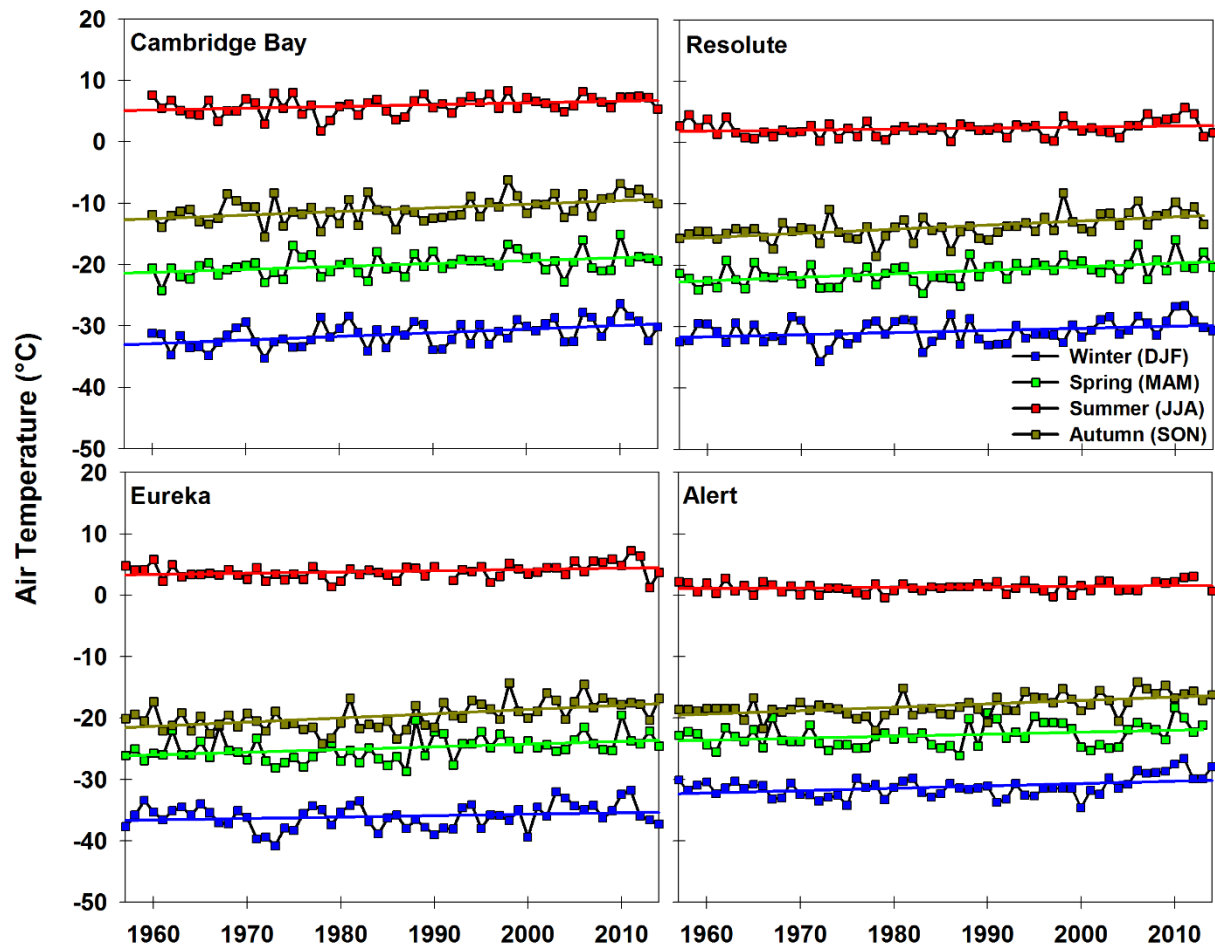
738  
 739 Figure 5. Time series and trend of observed mean October through May snow depth at the four  
 740 sites.

741  
 742  
 743  
 744  
 745  
 746



747  
 748 Figure 6. Weekly time series of ice thickness and snow depth at Eureka and Alert for (a) low  
 749 snow years and (b) high snow years.

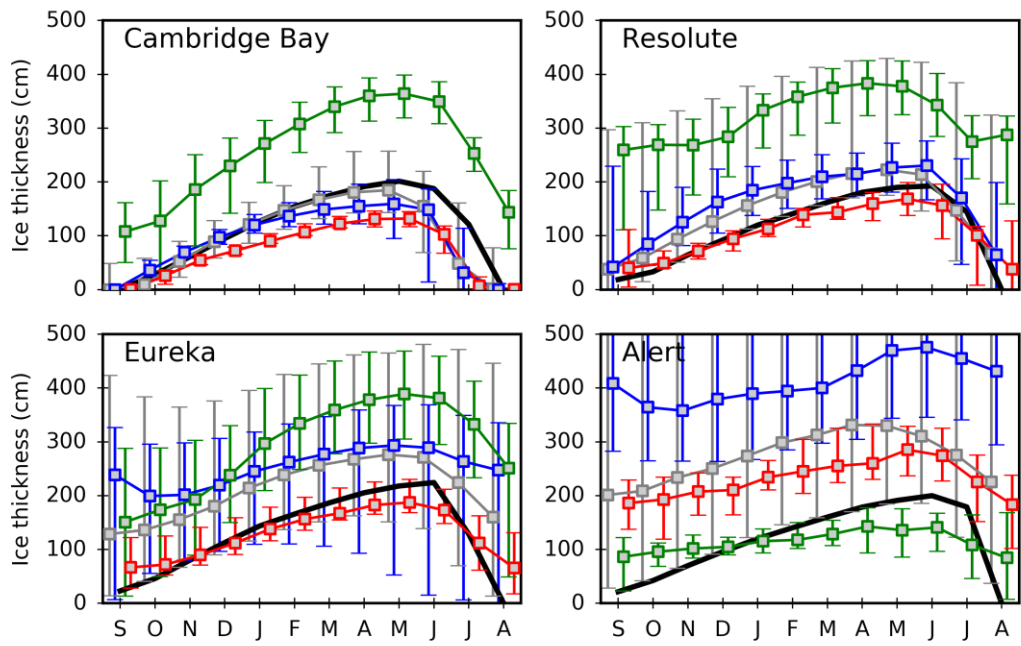
750  
 751  
 752  
 753



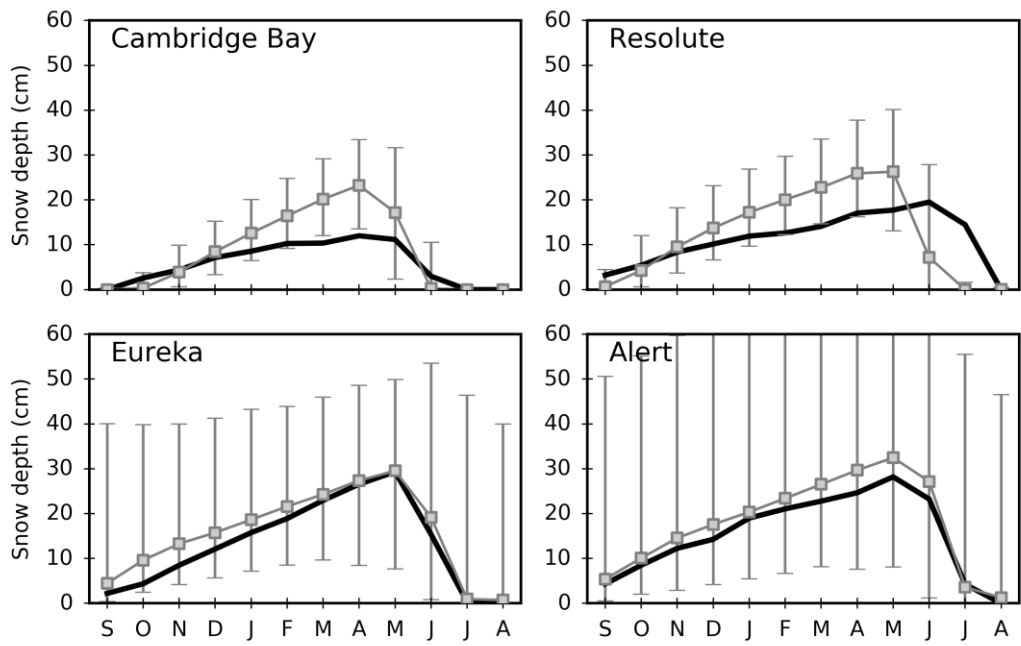
754  
 755 Figure 7. Time series of mean air temperature during winter (DJF), spring, (MAM), summer  
 756 (JJA) and autumn (SON) at the four sites.

757  
 758  
 759  
 760  
 761



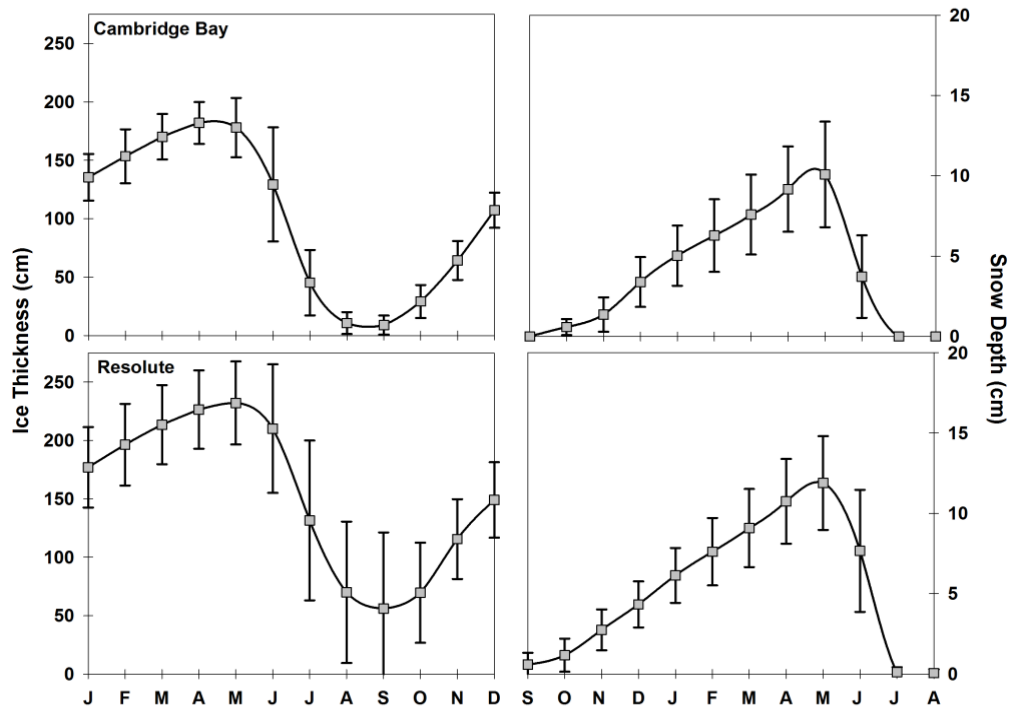


762  
 763 Figure 8. CMIP5 median sea ice thickness seasonal cycle (1955-2014) at stations (grey).  
 764 Observations from 2 (black). Median of ORA-IP models CGLORS, ORAP5.0, GLORYS2V3  
 765 (blue), ECCO-v4 (green) and UR025.4 (red). Whiskers indicate the 5th and 95th percentiles.  
 766  
 767  
 768  
 769  
 770



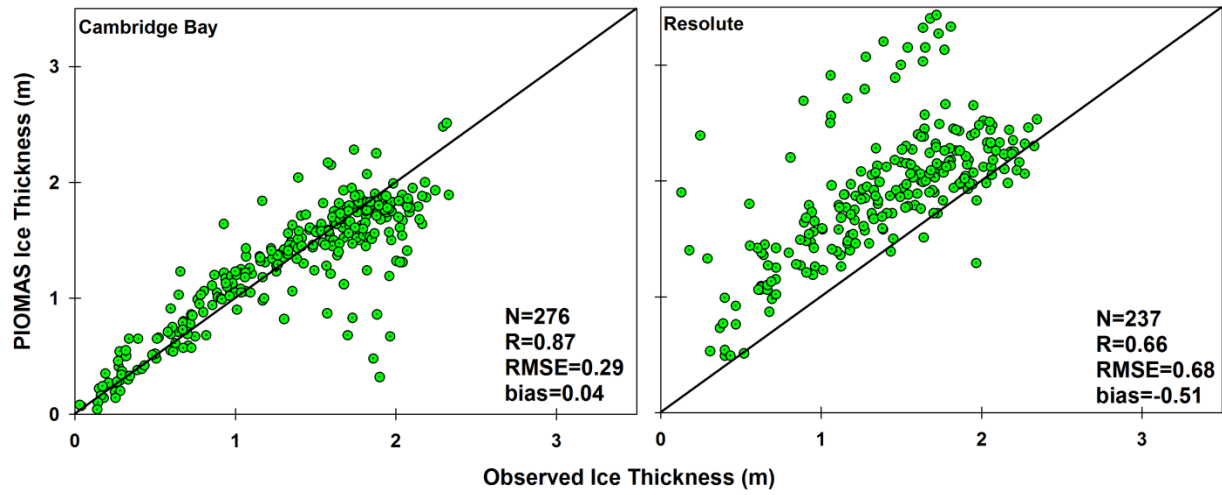
771  
 772  
 773  
 774  
 775  
 776  
 777  
 778  
 779  
 780  
 781  
 782  
 783  
 784  
 785  
 786  
 787  
 788  
 789  
 790  
 791  
 792  
 793  
 794  
 795  
 796  
 797

Figure 9. Same as Figure 8 for snow depth and only for CMIP5 models (grey) and observations (black).



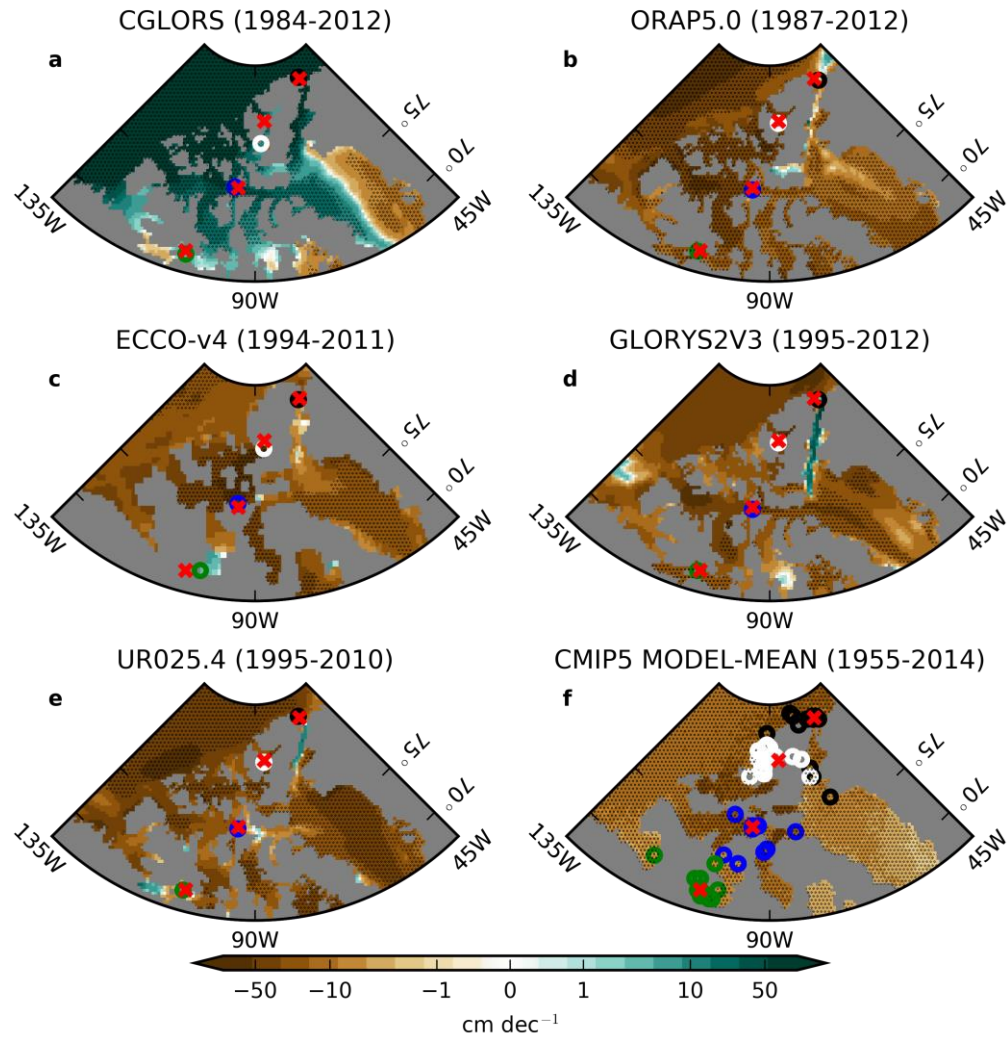
798 Figure 10. Seasonal cycle of observed mean ice thickness (left) and snow depth (right) from  
 799 PIOMAS at Cambridge Bay and Resolute (1979-2014).  
 800

801  
 802  
 803  
 804  
 805  
 806  
 807  
 808  
 809  
 810  
 811  
 812  
 813  
 814  
 815  
 816  
 817  
 818  
 819  
 820  
 821  
 822  
 823



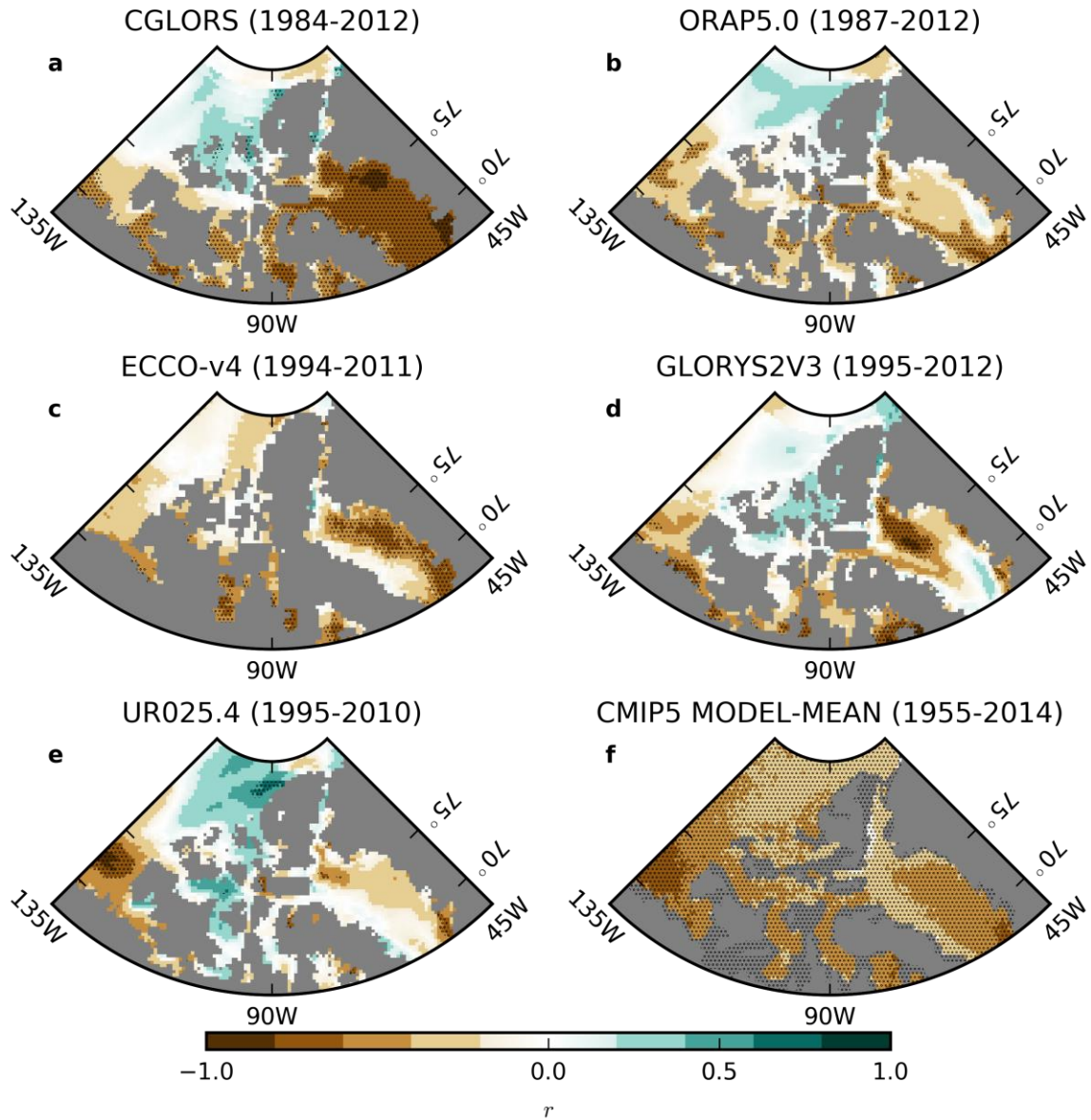
824  
825  
826  
827  
828  
829

Figure 11. Comparison of PIOMAS ice thickness with ice thickness observations from Environment Canada's ice thickness monitoring sites at Cambridge Bay and Resolute. The data covers the period 1979-2014.



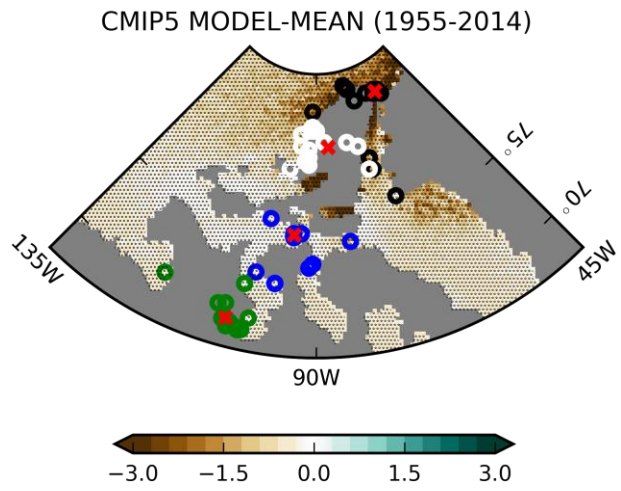
830  
 831  
 832  
 833  
 834  
 835  
 836  
 837  
 838  
 839  
 840  
 841  
 842  
 843  
 844  
 845  
 846  
 847

Figure 12. **a-e**: Maximum sea ice thickness trends in ORA-IP simulations. **f**: Same for CMIP5 MODEL-MEAN. From South to North, o's indicate Cambridge Bay (green), Resolute (blue), Eureka (white) and Alert (black) and x's indicate the corresponding measurement stations. In f, one o per model is shown." The stippling indicates p-values less than 0.05, corrected using the False Discovery Rate (FDR) method with a global pFDR-values less than 0.10 [Wilks, 2006]. The colorbar is linear from -10  $\text{cm dec}^{-1}$  to 10  $\text{cm dec}^{-1}$  and symmetric logarithmic beyond these values.



848  
 849  
 850  
 851  
 852  
 853  
 854  
 855  
 856  
 857  
 858  
 859  
 860  
 861  
 862

Figure 13. **a-c**: Pearson correlation of detrended maximum sea ice thickness in ORA-IP with detrended ONDJFMAM ERA-INTERIM 2m temperature. **f**: Same but for CMIP5 MODEL-MEAN. The stippling indicates p-values less than 0.05, corrected using the False Discovery Rate (FDR) method with a global pFDR-values less than 0.10 [Wilks, 2006].



863  
864  
865

Figure 14. Same as Figure 12f but for snow depth trends (ONDFJMM).